Nucleic Acids Research, 1997, Vol. 25, No. 15 **3017–3025**

Mechanisms of developmental regulation in *Trypanosoma brucei*: a polypyrimidine tract in the 3′-untranslated region of a surface protein mRNA affects RNA abundance and translation

Hans-Rudolf Hotz, Claudia Hartmann, Karin Huober, Michael Hug and Christine Clayton*

Zentrum für Molekulare Biologie, Universität Heidelberg, Im Neuenheimer Feld 282, D-69120 Heidelberg, Germany

Received April 28, 1997; Revised and Accepted June 12, 1997

ABSTRACT

Salivarian trypanosomes are extracellular parasites of mammals that are transmitted by tsetse flies. The procyclic acidic repetitive proteins (PARPs) are the major surface glycoproteins of the form of *Trypanosoma brucei* that replicates in the fly. The abundance of *PARP* mRNA and protein is very strongly regulated, mostly at the post-transcriptional level. The 3′-untranslated regions of two *PARP* genes are of similar lengths, but are dissimilar in sequence apart from a 16mer stem–loop that stimulates translation and a 26mer polypyrimidine tract. Addition of either of these *PARP* 3′-untranslated regions immediately downstream of a reporter gene resulted in developmental regulation mimicking that of PARP. We show that the *PARP* 3′-UTR reduces RNA stability and translation in bloodstream forms and that the 26mer polypyrimidine tract is necessary for both effects.

INTRODUCTION

The salivarian trypanosomes are unicellular parasites that live in the extracellular fluids of mammals and are transmitted by tsetse flies. The bloodstream forms evade the immune response by means of a thick coat of variant surface glycoprotein (VSG) (1,2). When they enter the tsetse fly midgut, many morphological and biochemical changes ensue as they transform into procyclic forms. One change is the replacement of VSG by the procyclic acidic repetitive protein (PARP or procyclin) (3,4).

Trypanosome gene expression is unusual in that nearly all protein coding genes so far investigated are transcribed in a polycistronic fashion (5,6). The precursor transcripts are processed into monocistronic mRNAs by 3′-polyadenylation and by 5′ addition of a capped 39 nt spliced leader. Polyadenylation is both spatially and temporally coupled to the *trans* splicing reaction. When *trans* splicing is inhibited, polyadenylation ceases (7). Usually several polyadenylation sites are used, scattered over a short region ~100 bases upstream of a *trans* splicing signal (8–11). Such signals commonly include a polypyrimidine tract with one or more acceptor AG dinucleotides up to ~80 bases downstream (12,13).

There is no evidence for any regulation of RNA polymerase II-catalysed transcription in trypanosomes. Developmental regulation of mRNA levels is determined post-transcriptionally; the sequences responsible are usually located in the 3′-untranslated region (3′-UTR) of the transcripts concerned (14–19). Transcription of the VSG and *PARP* genes is, in contrast, subject to some regulation (5,6,20–22), but the RNA polymerase responsible is probably RNA polymerase I (23–25). Expression of the *PARP* genes is regulated at several levels. Transcription is ~10-fold less active in bloodstream form trypanosomes than in procyclic forms (21,22,26), whereas PARP is undetectable in bloodstream forms. Indeed, expression of the antigenically invariant PARP at this stage would probably be lethal.

We have previously used a bicistronic vector bearing a *CAT* gene and hygromycin resistance (*HYG*) cassette to study developmental regulation mediated by 3′-UTRs placed downstream of the *CAT* gene. 3′-UTRs from genes expressed in bloodstream forms caused bloodstream form-specific CAT expression; 3′-UTRs from genes expressed in procyclic forms, such as *PARP* genes, caused procyclic form-specific CAT expression (17). Actin (*ACT*) mRNA levels are not developmentally regulated; *CAT* mRNA and CAT protein were correspondingly not regulated if the *CAT* gene bore an *ACT* 3′-UTR (17). Similar results have been reported for *PARP* and other 3′-UTRs placed downstream of *CAT* (18), luciferase (14) and phleomycin resistance genes (27,28).

Here we demonstrate that the sequence primarily responsible for PARP post-transcriptional regulation is a polypyrimidine tract that is conserved in all *PARP* gene 3′-UTRs. It acts by accelerating RNA turnover and inhibiting translation in bloodstream forms.

MATERIALS AND METHODS

Trypanosomes

Bloodstream trypanosomes (MiTat 1.2) and procyclic trypanosomes (derived from bloodstream Antat 1.1) were cultured and transfected and CAT assays performed as described (17,29). Hygromycin-resistant bloodstream trypanosome populations were generated by transfecting 10^7 trypanosomes with 10 μg

*To whom correspondence should be addressed. Tel: +49 6221 546876; Fax: +49 6221 545894; Email: cclayton@sun0.urz.uni-heidelberg.de

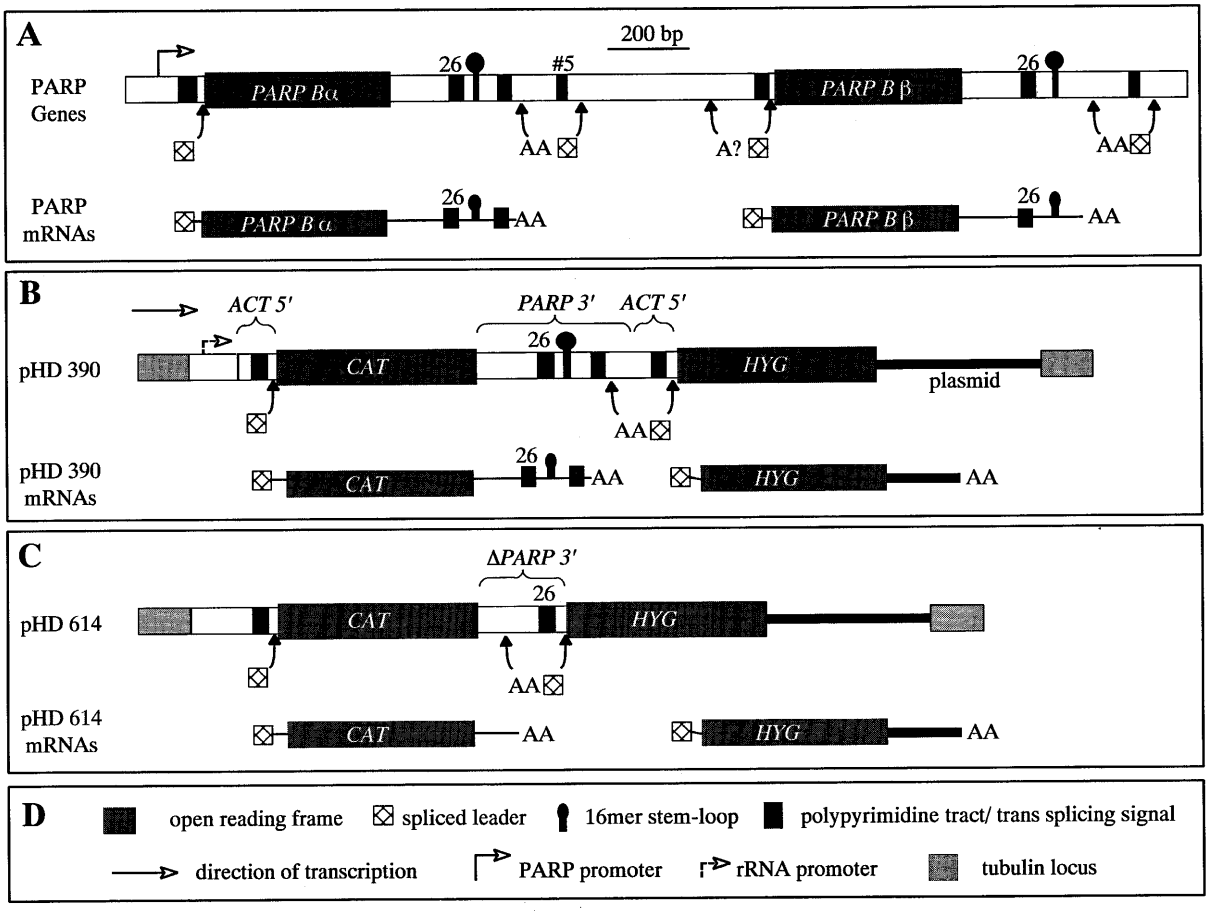

Figure 1. Map of a *PARP* B locus (**A**), pHD 390 (**B**), pHD 614 (**C**) and the corresponding mature mRNA products. Symbols are shown in (**D**). (A) The *PARP* promoter is shown at the extreme left and successive *PARP* open reading frames by dark stippled boxes. Polypyrimidine tracts that can, when placed upstream of an open reading frame, act as *trans* splicing signals, are shown as filled black blocks. Positions of *trans* splicing and the corresponding polyadenylation sites (AA) are indicated by the curved arrows. A hypothetical polyadenylation site is marked as A?. The polypyrimidine tract 26 is involved in developmental regulation and tract 5 specifies polyadenylation of the *PARP*α mRNA. The lollipop represents the translation-enhancing stem–loop (16mer) (34). (B) pHD 390 is shown linearized and integrated into the tubulin locus. The plasmid sequence (thick line) is not to scale. The locations of 3′- and 5′-UTRs and RNA processing signals are indicated. (C) pHD 614 and its transcripts.

plasmid DNA linearized within a tubulin targetting sequence and selected with 12.5 μg/ml hygromycin and the resulting populations were analysed as soon as sufficient parasites were available (22). Alternatively, plasmids were linearized within an rRNA targeting sequence and cloned by limiting dilution. CAT assays were performed at least three times on each population. Results were reproducible when independent populations were generated with the same plasmid.

Plasmid constructs

Plasmids for stable transfection were based on pHD 324 (17), a bicistronic construct containing *CAT* (with an *ACT* 3′-UTR) and hygromycin resistance (*HYG*) genes. Different 3′-UTRs or mutated forms of them were cloned downstream of *CAT*; pHD 390 (Fig. 1; 17) contains the *PARP*α 3′-UTR. The *PARP*β 3′-UTR (Fig. 2, pHD 440) was obtained by PCR with genomic DNA from procyclic AnTat 1 cells as template.

Mutations in the *PARP* 3′-UTRs were made either by exonuclease III deletion or PCR mutagenesis, followed by cutting and pasting of the resulting mutant fragments. Complete details, together with reconstructed sequences, are available from C.Clayton on request. *Trans* splicing activity was tested using plasmids derived from pHD 260 (9) with various *PARP* 3′-UTR fragments replacing the *ACT* 5′-UTR upstream of *CAT*.

RNA analysis

Total RNA was isolated using TRIzol reagent (Gibco Life Technologies Inc., Eggenstein). RNA from 3.3×10^6 (procyclic forms) or $1–5 \times 10^7$ (bloodstream form) cells was separated on formaldehyde gels and blotted onto Hybond N^+ membrane (Amersham, Braunschweig). In a few experiments mRNA was detected using enhanced chemiluminescence (ECL, Amersham). The exposed autoradiograms (30 s–5 h) were scanned (Agfa ARCUS II) and quantitated using NIH Image 1.52. In the other studies, including all turnover experiments, ^{32}P-labelled probes were used and bands quantitated using a phosphorimager (Molecular Dynamics). When compared, chemiluminescence and radioactive probing yielded quantitatively similar results.

For RNase protection analysis (30), a *CAT* cassette cloned into pBluscript II SK+ (Stratagene) was cleaved with *Nco*I and

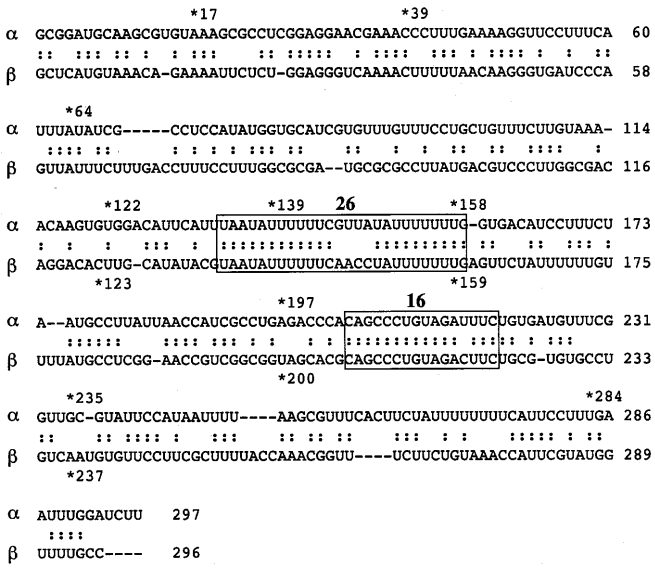

Figure 2. Sequence alignment of the *PARP*α and β 3′-UTRs used in this study. Nucleotide numbering starts at the first base after the stop codon and the sequences end at the major polyadenylation site. The last deleted nucleotides in the 5′ deletion constructs are indicated with asterisks. The (partially) homologous sequences are boxed and labelled 26 and 16. The Bβ sequence has six base changes relative to those previously published (50,51). Sequences tested as *trans* splicing signals were: for α, 125–203 or 118–203; for β, 127–206.

transcribed in the presence of [^{32}P]UTP to yield a 290 base product, which contained 56 bases that were not present in the mature *CAT* mRNAs. After RNase digestion the 234 base protected product was detected on sequencing gels, with appropriate controls.

The relationship between RNA half-lives and abundance were calculated using the formula:

$$v = \log 2(1/t_{½} + 1/t_{D})[\text{RNA}]$$

where $t_{½}$ is the measured half-life in non-growing cells and t_D is the mean division time of a growing population (8 h in bloodstream forms, 12 h in procyclics) (31). We assumed that the rate of degradation (v) of an mRNA equals its rate of synthesis.

Sequence alignments were done using align/lalign (32) and RNA folding assessed by MFOLD (33). Polyadenylation and splicing sites were determined by RT–PCR (9).

RESULTS

Sequence comparison of *PARP* 3′-UTRs

Trypanosoma brucei contains 8–12 *PARP* genes, arranged in direct tandem repeats containing two to three genes each (5). Figure 1A shows a simplified map of a *PARP* B locus with the corresponding mRNAs immediately below (*PARP* A loci are similar). Each locus bears an upstream (a) and a downstream (b) gene. The genes differ somewhat in the coding region but diverge in the 3′-UTRs. The untranslated regions, including both the intergenic regions and the 3′-UTRs of the mature mRNAs, include several polypyrimidine tracts. Some of these direct *trans* splicing of mature *PARP* mRNAs or of unstable, non-coding RNA intermediates. Others can also be shown to direct *trans* splicing if they are placed 5′ of a *CAT* open reading frame (9). Polypyrimidine tracts with known *trans* splicing activity are shown as filled boxes in Figure 1. Known linked upstream polyadenylation sites are also indicated.

An alignment of all *PARP* 3′-UTR sequences (e.g. *PARP* Bα and *PARP* Bβ, Fig. 2) reveals two conserved regions: a 16mer that is predicted to form a stem–loop and stimulates translation in procyclic forms (34) and a 26mer polypyrimidine tract (‘26’ in Figs 1–5). Secondary structure predictions for all available *PARP* 3′-UTR sequences (not shown) revealed no common features apart from the 16mer stem–loop; the 26mer poly(U) were not predicted to be involved in base pairing.

The *PARP* 3′-UTR mediates developmental regulation of mRNA levels and translation

To investigate the regulatory function of *PARP* 3′-UTRs, we used a vector designed to integrate into the tubulin locus (17; Fig. 1B). Downstream of a fragment from the tubulin locus (to enable targeted integration) is an rRNA promoter, which is not developmentally regulated (22). Next is an *ACT* 5′-UTR and splicing signal, followed by a *CAT* gene. The 3′-UTR downstream of *CAT* can be exchanged using unique restriction sites; it is from the *PARP* Bα locus in pHD 390 (Fig. 1B). Beyond this 3′-UTR is a second 5′ *trans* splicing signal and 5′-UTR from the *ACT* locus (17), then a hygromycin resistance (*HYG*) cassette. Unless otherwise noted, the plasmid was linearized, transfected into trypanosomes and hygromycin-resistant populations studied. Such populations are derived from at least 20 individual transformants containing one to three copies of the construct (17,22); their use obviates the need to perform independent copy number determinations for each plasmid tested. Transcription of *CAT* was probably mediated by RNA polymerase II reading through from upstream (17).

CAT mRNA with an *ACT* 3′-UTR (*CAT–ACT* 3′, pHD 324) shows no developmental regulation (17). Results for the *CAT–ACT* 3′ plasmid were therefore used as a control (100% value) throughout this study. Using the *PARP*α 3′-UTR, *CAT* mRNA and CAT protein levels were similar in procyclic forms to those seen with the *ACT* 3′-UTR; with the *PARP*β 3′-UTR CAT activity in procyclic forms was 2-fold less (not shown). In bloodstream forms (Fig. 3) CAT activity was suppressed >100-fold and *CAT* mRNA levels ~10-fold by the *PARP* 3′-UTRs. The discrepancy between the levels of *CAT–PARP* 3′ mRNA and the corresponding proteins indicates that the *PARP* 3′-UTRs not only reduce mRNA levels, but also adversely affect translation in bloodstream forms. Differentiation of bloodstream trypanosomes containing the *CAT–PARP* 3′ transgene into procyclic forms resulted in >100-fold up-regulation of CAT activity (to about half the final, procyclic level) within 48 h (35).

To check polyadenylation, *CAT–PARP* 3′ transcripts (from pHD 390) from procyclic forms or *CAT–PARP*Δ*26* 3′ (see below) transcripts from bloodstream forms were analysed by RT–PCR (9). In procyclics polyadenylation occurred either at the wild-type site or 12 bases upstream (two clones each). In bloodstream forms polyadenylation was at the wild-type site, except that one out of eight clones had poly(A) at position 173 (position ‘g’ in ref. 9).

Delineation of the sequences required for regulation

Deletion mutagenesis was used to localize sequences in the *PARP* 3′-UTRs that reduce bloodstream-form expression. Progressive 5′ deletions of the *PARP*α 3′-UTR up to position 139 (Fig. 3A) had marginal effects on CAT activity, but somewhat elevated *CAT*

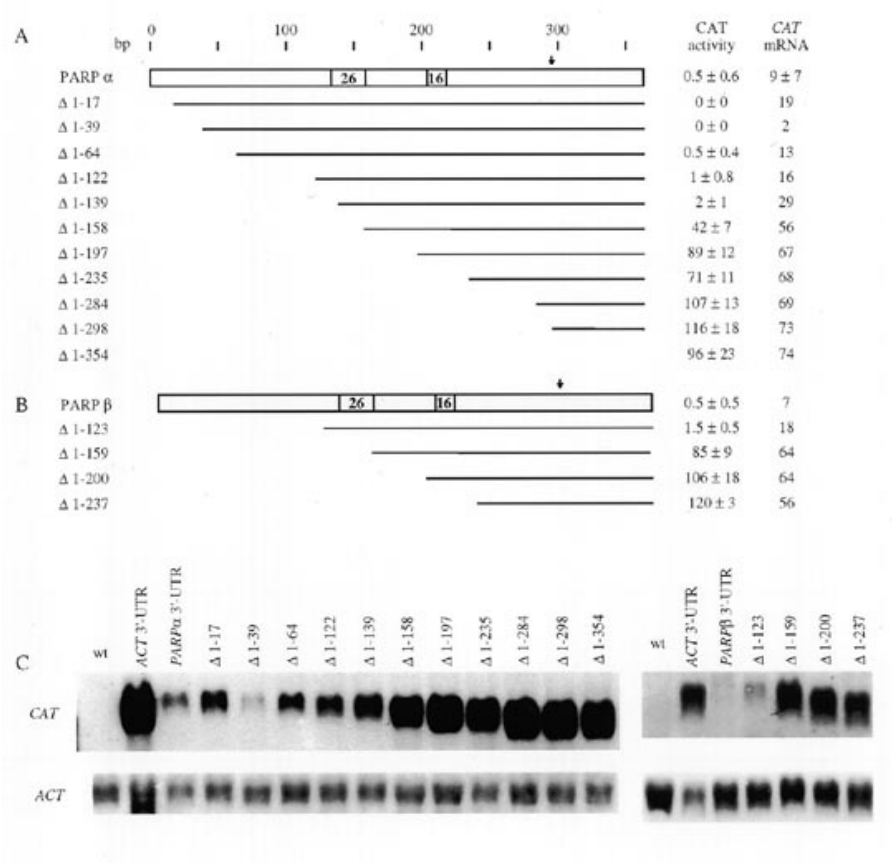

Figure 3. Deletion analysis of PARP 3′-UTRs: deletion from the 5′-side. Maps are of the *PARP*α (**A**) and β (**B**) 3′-UTRs. Arrow, wild-type polyadenylation site. Black lines indicate the sequence retained in each construct and the extent of deletions is indicated on the left. CAT activities for stably transformed bloodstream forms (mean ± SD of at least three independent transfections) are indicated as a percentage of the values obtained with pHD 324 (*CAT–ACT* 3′-UTR). CAT assays done with cell extracts from *hyg*^{R} cell populations were corrected according to the protein concentration. Quantitation of RNA, expressed as a percentage of the *CAT–ACT* 3′ control, from the blot (C) or from several experiments (for *PARP*α) are listed similarly. (**C**) Total RNA from 10^7 recombinant bloodstream cells, containing the deletion constructs indicated, was analysed by blot hybridization using a *CAT* probe. Hybridization with an *ACT* probe was done to standardize the amount of RNA. The extra, faster-migrating band in the *ACT* 3′-UTR lane, hybridized with the *ACT* probe, was due to redetection of the *CAT–ACT* 3′ mRNA.

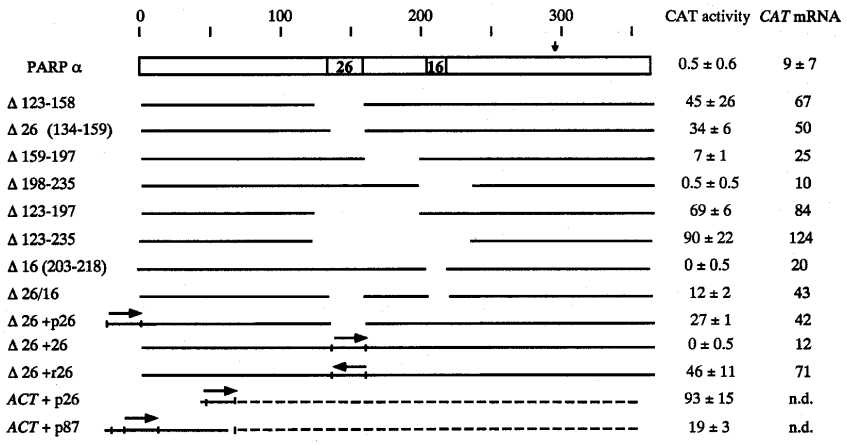

Figure 4. Internal deletion of the *PARP*α 3′-UTR. Details are as for Figure 3A. For internal deletions and replacements of the 26mer element, the inserted 26mer element is indicated as a short line flanked by two small bars and an arrow on top to indicate the orientation. The position of the 26mer sequence within the 87mer (*ACT* + p87) is also indicated by vertical bars. The *ACT* 3′-UTR is shown as an interrupted line (not to scale).

mRNA levels. Deletion 1–158 was the first to include the entire 26mer; suddenly CAT activity rose >100-fold to 42% of the *ACT* 3′-UTR control. The level of *CAT* mRNA from this mutant was about half that seen from the control. Further deletion (Δ1–197) yielded an additional 1.5–2-fold increase in CAT activity. Results for the *PARP*β 3′-UTR were quite similar (Fig. 3B); 5′ deletions

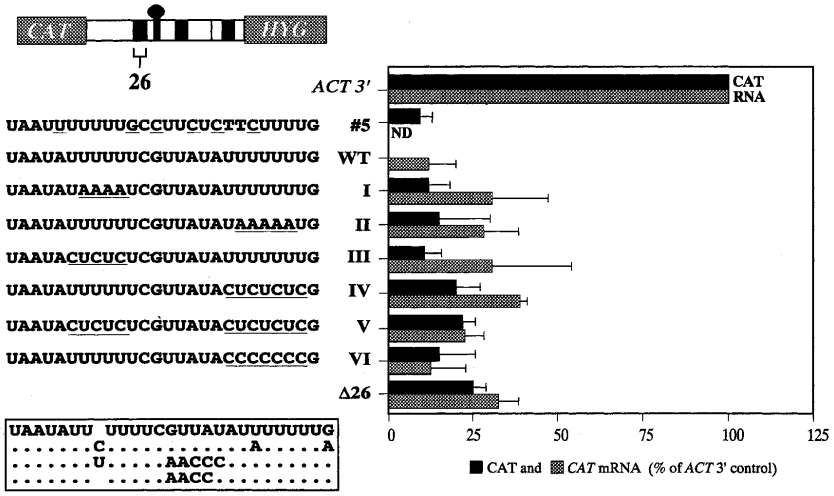

Figure 5. Function of *PARP*α 3′-UTRs with mutations in the 26mer. Mutations are indicated on the left. The box beneath the mutations shows the sequences of the 26mer in (from top to bottom) *PARP* Bα, *PARP* Aα, *PARP* Aβ and *PARP* Bβ 3′-UTRs; dots represent identity with the *PARP* Bα sequence. The CAT activities obtained from the mutated plasmids in permanently transformed bloodstream forms (black bars) and the corresponding levels of *CAT* mRNA (grey bars) are shown as mean ± SD for three or four independent transfection experiments.

that did not include the 26mer had little effect; as soon as the 26mer had gone (Δ1–159) CAT rose to 85%. Further deletions of the *PARP*β 3′-UTR yielded only marginal increases in RNA or protein (Fig. 3B).

These results suggested that the 26mer (134–159) was very important for regulation, although, for the *PARP*α 3′-UTR at least, the region immediately downstream (159–197) also played a role. Further deletions confirmed this interpretation. First we deleted 36 bases, including the 26mer, from the *PARP*α 3′-UTR (Fig. 4, Δ123–158). This restored 45% CAT activity, with a corresponding increase in *CAT* mRNA. Internal deletion of the downstream sequence (Δ159–197) independently increased CAT activity (to 7%) and *CAT* RNA (~2-fold) (Fig. 4). When both deletions were combined (Δ123–197) CAT was 69%. A mutant (Δ26/16) which has both the 26mer and the stem–loop deleted (Fig. 4, Δ134–159, Δ203–218) but retains bases 160–203 produced less *CAT* mRNA and CAT protein than the Δ123–235 mutant (Fig. 4), confirming that bases 160–203 reduce expression. None of the other sequences examined appeared important for down-regulation in bloodstream forms (Figs 3 and 4). The function of the 26mer was not dependent on its distance from the coding region (Fig. 3, Δ1–122 and data not shown) nor on the distance from the polyadenylation site (Fig. 4, Δ159–197 and Δ198–235).

The plasmids bearing deletions Δ134–159 and Δ123–158 (Δ26) were compared with the parent *PARP*α 3′-UTR plasmid by transient transfection assays in procyclic forms. No significant differences in CAT expression were found (not shown).

Precise deletion of the 26mer from the *PARP*β 3′-UTR resulted in 10% CAT expression and 50% RNA in bloodstream forms, relative to the *ACT* 3′-UTR control (not shown). Thus, here too, the 26mer was important for down-regulation, but other sequences must contribute.

The context of the 26mer is important

To examine the behaviour of the 26mer in more detail, we first replaced the 26mer of the *PARP*α 3′-UTR with a *Bgl*II site. Expression of CAT in bloodstream trypanosomes with this plasmid, yielding *CAT–PARP*Δ*26* 3′ RNA, was 34% of the *ACT* control (Δ26, Fig. 4). Returning the 26mer element to its original location (in the artificial *Bgl*II site) restored down-regulation if the 26mer was in the correct orientation (Δ26+26, Fig. 4). When the 26mer was placed immediately downstream of the *CAT* cassette, either upstream of *PARP*Δ*26* 3′ (Δ26+p26, Fig. 4) or upstream of *ACT* 3′, it did not suppress expression in bloodstream forms (*ACT* +p26, Fig. 4). When a larger segment of the *PARP*α 3′-UTR (117–203) was inserted between *CAT* and the *ACT* 3′-UTR, CAT activity was reduced 5-fold (*ACT* +p87, Fig. 4). Insertion of the inverted (antisense) 26mer had only minor effects (Δ26 +r26, Fig. 4 and data not shown).

In all constructs tested so far, polyadenylation of *CAT* mRNAs was directed by an *ACT* 5′ splicing sequence downstream (Fig. 1). To restore the *PARP*α 3′-UTR to its 'natural' context, we placed the complete *PARP* intergenic region (including the 3′-UTR) between the *CAT* and *HYG* cassettes. An equivalent construct with the Δ26 deletion was also tested. This change in the region downstream of the 3′-UTRs had no influence on the level of CAT expressed (not shown).

The conserved 16mer stem–loop has been shown to enhance translation in procyclic forms without influencing mRNA levels (34). Similar results were obtained for bloodstream forms: deletion of the 16mer from the Δ26 construct (Δ26/16) reduced CAT 3-fold, but the RNA level was unaffected (Fig. 4).

The 26mer can function as a *trans* splicing signal

To see if the *PARP*α and *PARP*β 26mers can act as *trans* splicing signals, we transferred appropriate segments of the 3′-UTRs (125–203 and 127–206 respectively, Fig. 2) to a 5′-UTR position, upstream of a *CAT* gene, and measured CAT activity after transient transfection. In the absence of a functional *trans* splicing signal, no CAT is produced (9,12). Both fragments were capable of directing CAT production in bloodstream and procyclic trypanosomes as efficiently as the *ACT* splice signal.

We next deleted from pHD 390 the segment from position 197, downstream of the 26mer in the *PARP*α 3′-UTR (Fig. 2) to the

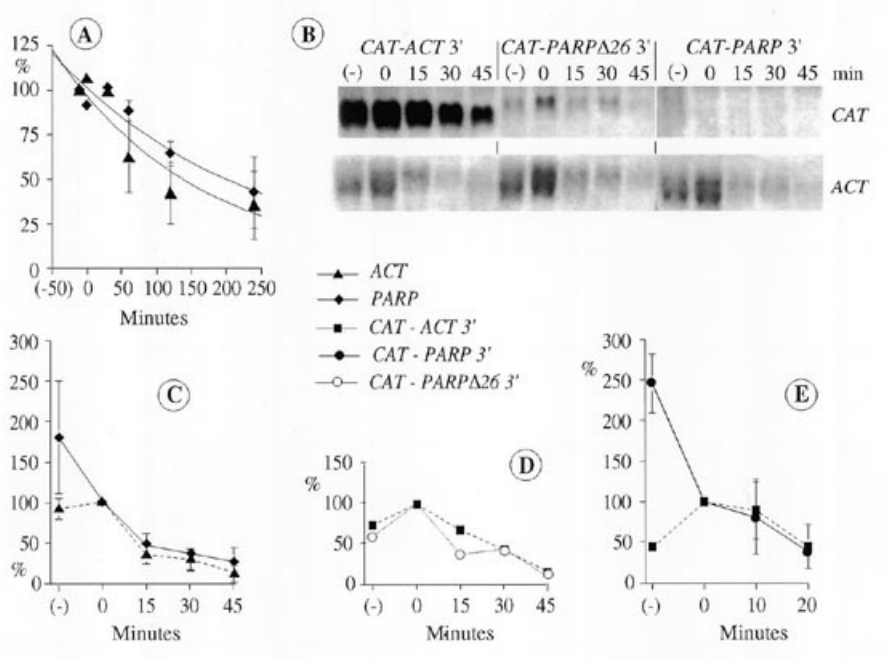

Figure 6. RNA turnover after transcription inhibition. At cell densities of 1–4 × 10^6 cells/ml (procyclics) or 1–1.8 × 10^6 cells/ml (bloodstream forms) cultures were subdivided into different flasks and drug (1 mg chloroquine/ml or 10 μg actinomycin D/ml) was added. (**A**) Procyclic trypanosomes. The (–) point is set to 100% and represents cells without drug. Results for five (*PARP*) or six (*ACT*) independent experiments are shown as arithmetic mean ± SD, except for the 0 and 30 min time points, which are the means of two experiments. Exponential curves were fitted by computer. (**B**–**E**) Bloodstream trypanosomes. Cells contained plasmids integrated in the tubulin locus (pHD 324, pHD 390 or pHD 523) except for (E), where data from lines containing similar plasmids integrated into the rRNA spacer (pHD 499 or pHD 663) were included. (B) Northern blot for cloned bloodstream trypanosomes expressing *CAT–ACT* 3′, *CAT–PARPΔ26* 3′ or *CAT–PARP* 3′ mRNAs. The time 0 panel represents cells where actinomycin D was added 1–5 min prior to centrifugation and the (–) lane shows cells that did not receive drug. Other lanes show RNA isolated from cells incubated for the indicated intervals relative to the *t* = 0 flask. The blot was hybridized with a *CAT* probe then stripped and rehybridized with a probe including an entire *ACT* gene including untranslated regions (this probe also hybridizes to *CAT–ACT* 3′ RNA). (C) *PARP* and *ACT* RNAs were quantified using data from the experiment shown in (A) and two other experiments using chloroquine as inhibitor. Results are arithmetic mean ± SD and are expressed as a percentage of the time 0 value. (D) *CAT* RNAs were quantified using data from the experiment shown in (A) for *CAT–PARPΔ26* and, in addition, for *CAT–ACT*, another experiment using chloroquine as inhibitor. (E) *CAT* RNAs were measured by RNase protection, using as probe a fragment from the 3′-end of *CAT*. Symbols with error bars represent mean and SD of three to five independent experiments, done using chloroquine as inhibitor. Half-lives were measured from computer-generated logarithmic plots.

beginning of the *HYG* gene (Fig. 1C, pHD 614). This forced use of the 26mer as a *trans* splicing signal for the *HYG* mRNA (Fig. 1C). Drug-resistant bloodstream trypanosomes were easily obtained. The *HYG* mRNA was spliced at the AG at position 197. Polyadenylation was 74 or 57 bases upstream of the 26mer and yielded *CAT* RNA and CAT activities similar to those from the *ACT* 3′-UTR control (not shown). Thus the 26mer must be within the mature 3′-UTR to down-regulate expression in bloodstream forms.

Replacement mutagenesis

We now mutated individual bases within the 26mer. The resulting CAT and *CAT* mRNA levels are shown in Figure 5. In this series of experiments *PARPΔ26* yielded CAT activity (black bars) and *CAT* mRNA (grey bars) of ~25% of the *ACT* 3′ control. All mutations of the 26mer, even those with only three transitions, affected regulation. CAT activity increased to at least 8% and, with one exception, RNA levels were doubled, attaining values similar to those from the Δ26 construct (Fig. 5). Mutant I and III 3′-UTRs yielded similar CAT activities to, but more RNA than, the mutant VI 3′-UTR. Mutant V has the sequence of the polypyrimidine tract that lies downstream of the *PARPα* polyadenylation site (9; see Fig. 1). This sequence is an active splice signal and mediates accurate *PARPα* polyadenylation (9), but is not as effective as the 26mer in reducing CAT expression and mRNA. The most interesting result was for mutant VI. This 3′-UTR appeared to have specifically lost the ability to down-regulate translation; the RNA level was reproducibly the same as for the wild-type *PARPα* 3′-UTR, but CAT expression was at least 10-fold higher.

mRNA turnover

Post-transcriptional regulation often operates at the level of RNA stability. We therefore compared turnover of selected mRNAs in cloned transgenic bloodstream and procyclic trypanosomes (see legends to Figs 6 and 7). RNA synthesis was inhibited using chloroquine (36) or actinomycin D (18) and the amounts of RNA assessed by blot hybridization or RNase protection. In all plots the negative time points show cells that were not drug treated and the zero time point represents cells that received drug 0–5 min before centrifugation (total time in the presence of drug 10–15 min). In procyclic forms the half-lives of *ACT* and *PARP* mRNAs were 1.5–2.5 h (Fig. 6A); results for *CAT–ACT* 3′ and *CAT–PARP* 3′ mRNAs were similar (not shown). RNAs with *PARP* 3′-UTRs were consistently slightly more stable than those with *ACT* 3′-UTRs, but the difference was not statistically significant. There was no difference between (–) and *t* = 0 samples.

All mRNAs tested were much less stable in bloodstream forms, so that the time taken to process the cells after drug treatment was significant relative to the half-life. A Northern blot demonstrating

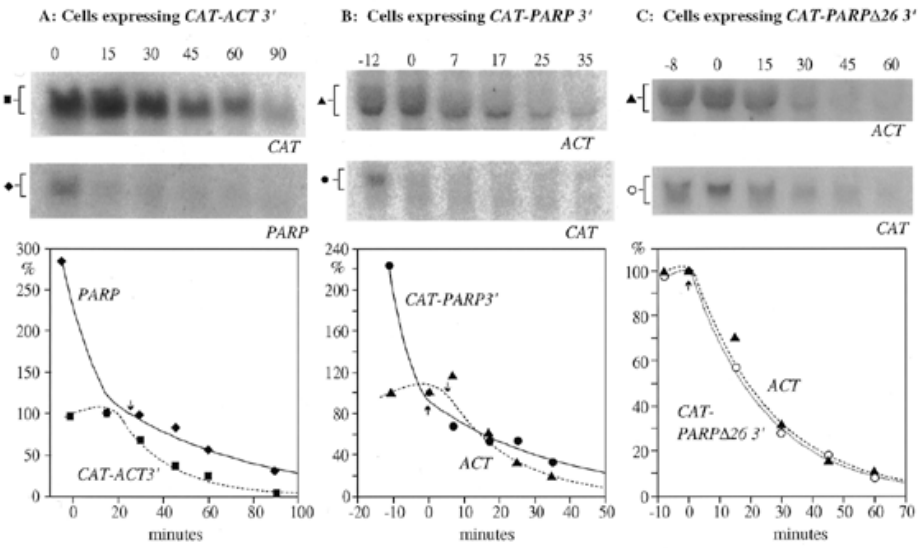

Figure 7. RNA turnover in bloodstream trypanosomes after splicing inhibition. Cloned cell lines bearing *CAT* genes integrated in the tubulin locus were treated with 1 µg/ml Sinefungin at densities of 1.2×10^6 cells/ml. Total RNA from 5×10^7 cells was loaded per lane. The experiment was done once only due to limited supplies of the drug. Time point 0 represents addition of drug immediately prior to centrifugation. Negative time points are samples without drug, the interval indicated being the sample processing time. The probe used to hybridize each Northern blot is indicated and quantitative results plotted beneath. Phosphorimager exposure times for *CAT* were 18 h for the *CAT–ACT* 3′ and *CAT–PARP*Δ*26* 3′ lines and 3 days for the *CAT–PARP* 3′ lines. Initial phosphorimager read-outs after subtraction of background were: (**A**) *CAT–ACT* 3′, 1946, *PARP,* 428; (**B**) *CAT–PARP*Δ*26* 3′, 787, *ACT,* 1860; (**C**) *CAT–PARP* 3′, 204 (background 91), *ACT,* 224. Curves preceding the small vertical arrow were fitted manually; beyond this point, exponential curves were fitted by computer and used to measure half-lives.

degradation after actinomycin D treatment is shown in Figure 6B. In this and every other experiment the control *ACT* mRNA and the *CAT–ACT* 3′ and *CAT–PARP*Δ*26* 3′ mRNAs increased immediately after drug addition, while PARP and *CAT–PARP* 3′ mRNA levels fell ~2-fold. Results for several independent experiments were combined for quantitation (Fig. 6C–E). *ACT* mRNA (Fig. 6C) had a half-life of 21 ± 12 min (mean ± SD, measured starting from the $t = 0$ time point) and the behaviour of the *CAT–ACT* 3′ and *CAT–PARP*Δ*26* 3′ transcripts was similar (Fig. 7D). In contrast, samples without drug contained twice as much *PARP* mRNA as samples in which drug was added just before centrifugation (Fig. 7B). From time point 0 onwards a low amount of *PARP* mRNA persisted; no accurate measurements of the turnover of this residual *PARP* RNA were possible because of its low abundance.

To facilitate detection of the *CAT–PARP* 3′ mRNA we used RNase protection, with a probe from the 3′-end of the *CAT* gene. Results for the *CAT–ACT* 3′ mRNA were similar to those obtained by Northern blot (compare Fig. 6D and E). The *CAT–PARP* 3′ mRNA, like the *PARP* mRNA, declined precipitously immediately after drug addition (compare Fig. 7C and E). The results for *CAT–ACT* 3′ mRNA, *CAT–PARP* 3′ mRNA and *CAT–PARP*Δ*26* 3′ mRNA were confirmed using a probe from the 5′-end of the *CAT* gene (35).

It was possible that the biphasic kinetics of *CAT–PARP* mRNA decay was an artifact of the use of actinomycin D or chloroquine to inhibit transcription. Pulse-chase analysis with [^{3}H]adenine cannot be used because the added nucleotide takes 1 h to equilibrate with internal pools (37). As an alternative, we inhibited RNA maturation using Sinefungin, which prevents methylation of the spliced leader RNA (38). (We are grateful to Dr E.Ullu, Yale University, New Haven, CT, for suggesting this approach.) Northern blots and quantitations are shown in Figure 7. In all cases, the declines in mature RNAs shown were accompanied by the appearance and accumulation of one or two larger mRNA species (not shown in Fig. 7), which presumably are unprocessed precursors. The mean length of all mature transcripts decreased during the incubation. The *ACT* (Fig. 7B and C) and *CAT–ACT* 3′ (Fig. 7A) mRNAs were initially stable. This lag before degradation was seen previously for tubulin mRNA (38) and was interpreted as a short period of continued splicing, using residual pre-synthesized spliced leader supplies. However, *PARP* (Fig. 7A) and *CAT–PARP* 3′ (Fig. 7B) mRNAs declined 2–3-fold immediately after drug addition. This observation both confirms the results previously seen using actinomycin D and chloroquine and suggests that the available pool of pre-synthesized spliced leader may be smaller than previously supposed. As before, the *PARP* and *CAT–PARP* 3′ mRNAs that remained after the initial rapid decrease were as stable as *ACT* and *CAT–ACT* 3′ mRNAs. A faint smear below the band for the mature *CAT–PARP* 3′ mRNA may be a degradation product. The *CAT–PARP*Δ*26* 3′ mRNA behaved similarly to the *CAT–ACT* 3′ mRNA (Fig. 7C).

In summary, in bloodstream forms most *PARP* and *CAT–PARP* 3′ mRNA is destroyed immediately after it is formed, in a process dependent on the 26mer.

DISCUSSION

Sequence requirements for regulation

We have shown that two *PARP* 3′-UTRs mediate >10-fold down-regulation of *CAT* mRNA levels and >100-fold down-regulation of CAT activity in bloodstream trypanosomes. The 10-fold post-transcriptional regulation of mRNA levels is consistent with the 100-fold *PARP* mRNA regulation observed in these trypanosomes (22), as *PARP* transcription is 5–10-fold less active in bloodstream

forms than in procyclics (22). A conserved polypyrimidine tract (26mer) is important in this regulation. The function of the 26mer did not depend on its distance from the coding region or from the polyadenylation site, but it had to be present in the mature mRNA, as transcripts polyadenylated 5′ of the 26mer were abundant and well-translated in bloodstream forms. Interactions with other sequences in the 3′-UTR were not essential, but in the *PARP*α 3′-UTR additional regulatory elements were present immediately downstream. The ability of the 26mer to suppress expression in bloodstream forms was dependent on context. It could not repress expression when placed at the 5′-ends of the *ACT* 3′ or *PARP*α*Δ26* 3′-UTRs. Perhaps, when the 26mer is moved from its normal location its function is overridden by other sequences that either exert a positive influence on the RNA level or form secondary structures that preclude 26mer function.

Although the 26mer is U-rich, it is poorly homologous to the UA-rich nonamer that is implicated in RNA decay in mammalian cells (39,40). Trypanosomes diverged so early in eukaryotic evolution that the vague resemblance between the two sequences is most likely fortuitous. Also, the first six bases (UAAUAU) of the 26mer were not required for repression (Δ1–139, Fig. 3). In contrast, all mutations of the two pyrimidine tracts within the 26mer affected activity. As few as three base changes in these portions were sufficient to increase CAT expression and *CAT* mRNA to levels approaching, or equivalent to, those seen when the entire 26mer was deleted (Fig. 5). Polypyrimidine tracts are common in trypanosome 3′-UTRs, whether or not the mRNAs are abundant in bloodstream forms, so recognition of this particular one by regulatory mechanisms must be very sequence specific.

mRNA is less stable in bloodstream forms than in procyclic forms

Ehlers *et al*. (41) measured RNA turnover in trypanosomes by pulse-chase labelling with [^{3}H]adenine. They found that total poly(A)$^+$ RNA turned over faster in bloodstream forms than in procyclics. The estimated half-life of tubulin mRNA, which shows little developmental regulation, was 1.4 h in bloodstream forms and 7 h in procyclic forms (41). These values were probably artifactually long due to the large ATP pool (36,37). Using RNA synthesis inhibitors, we found that the half-life of *ACT* mRNA was 20 min in bloodstream forms, but 90 min in procyclics.

The levels of *ACT* mRNA, as a proportion of total mRNA, are approximately the same in bloodstream forms and procyclic forms (42). How can this be when the degradation rates differ nearly 5-fold? Firstly, we routinely obtain two to three times less RNA from bloodstream trypanosomes than from procyclic forms. Secondly, bloodstream forms grow at 37°C and procyclics at 27°C; perhaps everything: transcription, processing and degradation, is faster at the higher temperature.

The 26mer influences mRNA turnover

Previous reports have indicated regulation of trypanosomatid RNAs through accelerated or delayed turnover. Experiments in which *VSG* 5′- and 3′-UTRs were linked to a *CAT* gene yielded results suggesting that these sequences are capable of reducing mRNA levels in procyclic forms (18,43), with some effects on RNA stability (18). Regulation of gene *A2* mRNA in *Leishmania donovani* was also shown to be mediated by elements in the 3′-UTR that affected RNA stability (44), the data being consistent with biphasic mRNA decay kinetics.

Our results indicate that accelerated turnover contributes to the low abundance of *PARP* or *CAT–PARP* 3′ mRNAs in bloodstream forms. After inhibition of mRNA synthesis, most *CAT–PARP* 3′ mRNA was degraded within 10 min. The *CAT–PARPΔ26* 3′ mRNA, in contrast, behaved like *CAT–ACT* 3′ mRNA, indicating that the 26mer was required for rapid degradation. After 10–15 min the rates of degradation of all these RNAs were indistinguishable. The biphasic kinetics of *PARP* and *CAT–PARP* 3′ mRNA degradation suggest that there are two RNA subpopulations. Perhaps most of the newly synthesized RNA is degraded in the nucleus, while the portion that escapes into the cytosol is more stable? So far our attempts to test this hypothesis have been frustrated by an inability to detect *CAT–PARP* 3′ mRNAs after cell fractionation. In one experiment (Fig. 7) a possible degradation intermediate of *CAT–PARP* 3′ mRNA was seen. We do not know the structure of this band. All mRNAs investigated showed a gradual decrease in size after inhibition of RNA synthesis. This would be consistent with shortening of the poly(A) tail prior to degradation, as is seen in other eukaryotes (45,46).

Regulation of mRNA processing or export?

In mammalian cells and yeast binding of splicing factors to unprocessed RNAs can inhibit their export from the nucleus, leading to rapid degradation (47,48). It therefore seemed possible that the U-rich 26mer was affecting RNA abundance by this mechanism. When a segment including both the 26mer and the downstream sequence up to the next AG dinucleotide was placed upstream of an open reading frame (*CAT* or *HYG*), *trans* splicing activity was indeed detected. However, the *trans* splicing ability was not developmentally regulated and preliminary mutation results (49) have yielded no evidence so far for any correlation between *trans* splicing potentiality and the ability to reduce mRNA levels.

Translation

Bloodstream forms contain some mature *PARP* mRNA, but PARP is undetectable because the 26mer represses translation. Surveying the results from all mutants, an increase in CAT activity to a level significantly above background (2% and more) usually correlated with a rise in the amount of RNA to >20%; RNA levels of >35% yielded CAT activities >25%. One mutation of the 26mer abolished translational repression without affecting the level of mRNA (Fig. 5), suggesting involvement of separate factors (or separate specificities within one factor) that interact with the 26mer. To further investigate post-transcriptional regulation of PARP expression it will be necessary to identify and characterize these factors.

ACKNOWLEDGEMENTS

We are indebted to Elisabetta Ullu (Yale University, New Haven, CT) for suggesting the use of Sinefungin for RNA degradation studies and kindly donating some of her remaining supplies for this purpose (the drug is no longer commercially available). We thank Drs Timothy Nilson (Case-Western Reserve University, USA), Christian Tschudi (Yale University, New Haven, CT), Stephan Krieger, Martin Eilers Patrick Lorenz and Henriette Irmer (ZMBH) for discussions or helpful comments on the

manuscript. Oligonucleotides were synthesized by the ZMBH oligonucleotide synthesis facility. This work was supported by the Deutsche Forschungsgemeinschaft.

REFERENCES

1 Pays,E., Vanhamme,L. and Berberof,M. (1994) *Annu. Rev. Microbiol*., **48**, 25–52.
2 Cross,G.A.M. (1990) *Annu. Rev. Immunol*., **8**, 83–110.
3 Roditi,I., Schwartz,H., Pearson,T.W., Beecroft,R.P., Liu,M.K., Richardson,J.P., Büring,H.-J., Pleiss,J., Bülow,R., Williams,R.O. and Overath,P. (1989) *J. Cell Biol*., **108**, 737–746.
4 Clayton,C.E., Fueri,J. and Mowatt,M. (1990) In Wang,C.C. (ed.), *Molecular and Immunological Aspects of Parasitism*. American association for the Advancement of Science, New Orleans, LA, pp. 55–64.
5 Vanhamme,L. and Pays,E. (1995) *Microbiol. Rev.*, **59**, 223–240.
6 Graham,S.V. (1995) *Parasitol. Today*, **11**, 217–223.
7 Ullu,E., Matthews,K.R. and Tschudi,C. (1993) *Mol. Cell. Biol*., **13**, 720–725.
8 LeBowitz,J.H., Smith,H.Q., Rusche,L. and Beverley,S.M. (1993) *Genes Dev.*, **7**, 996–1007.
9 Hug,M., Hotz,H.R., Hartmann,C. and Clayton,C.E. (1994) *Mol. Cell. Biol*., **14**, 7428–7435.
10 Matthews,K.R., Tschudi,C. and Ullu,E. (1994) *Genes Dev.*, **8**, 491–501.
11 Schürch,N., Hehl,A., Vassella,E., Braun,R. and Roditi,I. (1994) *Mol. Cell. Biol*., **14**, 3668–3675.
12 Huang,J. and van der Ploeg,L.H.T. (1991) *EMBO J*., **10**, 3877–3885.
13 de Lafaille,M.A.C., Laban,A. and Wirth,D.F. (1992) *Proc. Natl. Acad. Sci. USA*, **89**, 2703–2707.
14 Hug,M., Carruthers,V., Sherman,D., Hartmann,C., Cross,G.A.M. and Clayton,C.E. (1993) *Mol. Biochem. Parasitol*., **61**, 87–96.
15 Ramamoorthy,R., Swihart,K.G., McCoy,J.J., Wilson,M.E. and Donelson,J.E. (1995) *J. Biol. Chem*., **270**, 12133–12139.
16 Blattner,J. and Clayton,C.E. (1995) *Gene*, **162**, 153–156.
17 Hotz,H.-R., Lorenz,P., Fischer,R., Krieger,S. and Clayton,C.E. (1995) *Mol. Biochem. Parasitol*., **75**, 1–14.
18 Berberof,M., Vanhamme,L., Tebabi,P., Pays,A., Jefferies,D., Welburn,S. and Pays,E. (1995) *EMBO J*., **14**(12), 2925–2934.
19 Nozaki,T. and Cross,G.A.M. (1995) *Mol. Biochem. Parasitol*., **75**, 55–68.
20 Rudenko,G., Blundell,P.A., Taylor,M.C., Kieft,R. and Borst,P. (1994) *EMBO J*., **13**, 5470–5482.
21 Vanhamme,L., Berberof,M., Le Ray,D. and Pays,E. (1995) *Nucleic Acids Res*., **23**, 1862–1869.
22 Biebinger,S., Rettenmaier,S., Flaspohler,J., Hartmann,C., Peña-Diaz,J., Wirtz,L.E., Hotz,H.R., Barry,J.D. and Clayton,C.E. (1996) *Nucleic Acids Res*., **24**, 1202–1211.
23 Chung,H.-M., Lee,M.G.-S. and Van der Ploeg,L.H.T. (1992) *Parasitol. Today*, **8**, 414–418.
24 Chung,H.-M.M., Lee,M.G.-S., Dietrich,P., Huang,J. and van der Ploeg,L.H.T. (1993) *Mol. Cell. Biol*., **13**, 3734–3743.
25 Janz,L. and Clayton,C. (1994) *Mol. Cell. Biol*., **14**, 5804–5811.
26 Rudenko,G., Lee,M.G.-S. and Van der Ploeg,L.H.T. (1992) *Nucleic Acids Res*., **20**, 303–306.
27 Hug,M. (1994) Dissertation, Universität Heidelberg, Heidelberg, Germany.
28 Häusler,T. and Clayton,C.E. (1996) *Mol. Biochem. Parasitol*., **76**, 57–72.
29 Wirtz,L.E., Hartmann,C. and Clayton,C. E. (1994) *Nucleic Acids Res*., **22**, 3887–3894.
30 Gilman,M. (1993) In Ausubel,F.M., Brent,R.E., Kingston,R.E., Moore,D.D., Seidman,J.G., Smith,J.A. and Struhl,K. (eds), *Current Protocols in Molecular Biology*. Greene Publishing Associates and John Wiley and Sons, Boston, MA.
31 Belasco,J.G. and Brawerman,G. (1993) In Belasco,J.G. and Brawerman,G. (eds), *Control of Messenger RNA Stability*. Academic Press, San Diego, CA, pp. 475–494.
32 Huang,X. and Miller,W. (1991) *Adv. Appl. Math*., **12**, 373–381.
33 Jaeger,J.A., Turner,D.H. and Zuker,M. (1989) *Proc. Natl. Acad. Sci. USA*, **86**, 7706–7710.
34 Hehl,A., Vassella,E., Braun,R. and Roditi,I. (1994) *Proc. Natl. Acad. Sci. USA*, **91**, 370–374.
35 Hotz,H.-R. (1996) Dissertation, Universität Heidelberg, Heidelberg, Germany.
36 Laird,P.W., ten Asbroek,L.M.A. and Borst,P. (1987) *Nucleic Acids Res*., **15**, 10087–10103.
37 Laird,P.W., Zomerdijk,J.C.B.M., de Korte,D. and Borst,P. (1987) *EMBO J*., **6**, 1055–1062.
38 McNally,K.P. and Agabian,N. (1992) *Mol. Cell. Biol*., **12**, 4844–4851.
39 Chen,C.-Y.A. and Shyu,A.-B. (1995) *Trends. Biochem. Sci*., **20**, 465–470.
40 Zubiaga,A.M., Belasco,J.G. and Greenberg,M.E. (1995) *Mol. Cell. Biol*., **15**, 2219–2230.
41 Ehlers,B., Czichos,J. and Overath,P. (1987) *Mol. Cell. Biol*., **7**, 1242–1249.
42 Ben Amar,M.F., Pays,A., Tebabi,P., Dero,B., Seebeck,T., Steinert,M. and Pays,E. (1988) *Mol. Cell. Biol*., **8**, 2166–2176.
43 Zomerdijk,J.C.B.M., Ouellette,M., ten Asbroek,A.L.M.A., Kieft,R., Bommer,A.M.M., Clayton,C.E. and Borst,P. (1990) *EMBO J*., **9**, 2791–2801.
44 Charest,H., Zhang,W.-W. and Matlashewski,G. (1996) *J. Biol. Chem*., **271**, 17081–17090.
45 Caponigro,G. and Parker,R. (1996) *Microbiol. Rev.*, **60**, 233–249.
46 Brawerman,G. (1993) In Belasco,J.G. and Brawerman,G. (eds), *Control of Messenger RNA Stability*. Academic Press, San Diego, CA, pp. 149–160.
47 Legrain,P. and Rosbash,M. (1989) *Cell*, **57**, 573–583.
48 Chang,D.D. and Sharp,P.A. (1989) *Cell*, **59**, 789–795.
49 Huober,K. (1996) Diploma thesis, University of Heidelberg, Heidelberg, Germany.
50 Mowatt,M.R. and Clayton,C.E. (1988) *Mol. Cell. Biol*., **8**, 4055–4062.
51 Koenig-Martin,E., Yamage,M. and Roditi,I. (1992) *Mol. Biochem. Parasitol*., **55**, 135–145.